International Journal of New Horizons in Physics

http://dx.doi.org/10.18576/ijnhp/070105

Study on Structural/Magnetic Properties Correlation of Multiferroic Perovskite Bismuth Ferrite ($BiFeO_3$)

M. I. Marzouk[1], *H. M. Hashem*[1], *S. Soltan*[1,2] *and A. A. Ramadan*[1]

[1]Department of physics, Faculty of Science, Helwan university, Cairo, Egypt.
[2]Max- Planck institute for solid state research, Stuttgart, Germany.

Received:21 Oct. 2019,Revised: 22 Nov.2019,Accepted:24 Dec.2019.
Publishedonline:1 Jan 2020.

Abstract: The structural characterization and magnetic investigations of perovskite bismuth ferrite were studied using X-ray diffraction (XRD) and superconducting quantum interference device (SQUID) magnetometer, respectively. Raman spectroscopy investigation was performed in order to confirm the obtaining of bismuth ferrite ($BiFeO_3$) structural phase. The optimum conditions for the synthesis of bismuth ferrite sample was found to be 600 ºC and 800 ºC /6 hours for the first and second sintering stage, respectively. The sample has been melted as sintering temperature ascended above of 800 ºC. Rietveld refinement was applied for quantitative phase analysis. The Neel temperature of bismuth ferrite was 538 K as determined from the electrical resistivity measurement as a function of temperature. A magnetic phase transition from metallic (Para magnetic) into insulator (Anti ferromagnetic) state was observed at the Neel temperature. A room temperature weak ferromagnetic behaviour is observed in $BiFeO_3$ (BFO) sample that is referred to the spin canting configuration.

Keywords: Structural, Magnetic, Bismuth Ferrite.

1 Introduction

Bismuth ferrite or bismuth iron oxide ($BiFeO_3$) is a multiferroic material, which contains an overlapping of the ferroelectric and (Anti) ferromagnetic orders at room temperature. The correlations between electric dipole moment and magnetization leads to an interesting functionality called magneto-electric coupling. The synthesize process of bismuth ferrite ($BiFeO_3$) phase is very complicated due to its perovskite structure, and mostly in ceramic form the formation of pure phase is very difficult especially if it started by raw oxides [1,2]. The Neel temperature of bismuth ferrite was reported at 643, 650 and 673K [1-3]. The magnetoelectric coupling allows to the occurrence of several applications in functional devices as well as spintronics applications [2,3].Selbach et al. [4], prepared $BiFeO_3$ phase by the wet chemical rout method and they reported that the bismuth ferrite ($BiFeO_3$) phase decomposes to other impurity phases: $Bi_{25}FeO_{39}$ and $Bi_2Fe_4O_9$ in the temperature interval of (720-1040) K. In presence of magnetoelectric coupling, it means that the magnetization of material can be electric field controlled and the electric polarization can be magnetic field controlled as well due to the interaction between ferroelectric and antiferromagnetic orders. The magnetoelectric coupling in bismuth ferrite was referred to the ferroelectric distortion that appears in the perovskite structure, which then leads toa switching of magnetization through spin canting as reported by Ederer and Fennie [5]. The study aims to optimize the preparation parameters of bismuth ferrite ($BiFeO_3$) phase by solid-state reaction. Correlation of structure characteristics with the electric and magnetic properties will be considered.

2 Experimental

The synthesis process of perovskite bismuth ferrite ($BiFeO_3$) phase was prepared by conventional solid- state reaction method. The starting materials of raw oxides of bismuth oxide (III) (99.99%, sigma Aldrich) and iron oxide (III) (99.99%, Sigma Aldrich) were mixed together in a stoichiometric ratio (1:1).The mixture was then grinded in an agate mortar for 15 min in presence of ethyl alcohol to increase the homogeneity of mixture. The mixture was then sintered in an air furnace with two sintering stages at different temperatures for 6 hr:the first sintering stage at 500 ºC and 600 ºC and the second stage at 720ºC, 800ºC and 820 ºC. Structural characterization of samples was performed using X-raydiffractometer (EMPYREAN,PANalytical) at room temperature with Cu-K_α radiation(λ=1.54Å) at operating voltage and current of 45kVand 30 mA. The electrical measurements were investigated using high current source (Keithley 238) in the

*Correspondingauthore-mail:

temperature range of 300-800K. Magnetic properties were studied via superconducting quantum interference device (SQUID), MPMS3 quantum design, USA.

3 Results and Discussions

A phase optimization process based on different temperatures at two sintering stages have been carried out to select the optimum condition for obtaining the $BiFeO_3$-phase.Figure (1) shows the X-ray diffractograms of the synthesized bismuth iron oxide samplesafterthe first sintering stage.The phase identification based on JCPDS cards illustrates that the sintered samples contains the main proposed phase ($BiFeO_3$) in addition to two parasitic secondary phases ($Bi_{25}FeO_{40}$ and $Bi_2Fe_4O_9$). As the temperature is ascended from 500 ºC to 600ºC,the peaks of the secondary $Bi_2Fe_4O_9$ phase were disappear as clearly shown in Figure (1b).On the other hand, the peak intensities of $BiFeO_3$ and$Bi_{25}FeO_{40}$ phases are increased specially of the parent phase. Thus,the optimum conditions for the first sintering stage are 600ºCwith sintering time of 6 hrs.

On the other hand, it was also shown that as the first sintering temperature ascends from 500 to 600 ºC, the diffraction peaks are shifted to higher 2θ-angles.

The direction of the shift indicates a decrease in unit cell volume, which seems to be due to volatile nature of Bi. Synthesis of BFO at high temperatures results in depletion of bismuth. This creates bismuth vacancies (VBi), which leads to the formation of oxygen vacancies (VO) or multiple valance of Fe ($Fe^{3+}$to Fe^{2+})to maintain charge neutrality in BFO ceramics [6-9]. XPS results confirm the single valance state of Fe in undoped and Ba doped samples [10-11]. Therefore, the solid- state reaction at high temperature results in the formation of V_{Bi} and V_O as described by the following Kroger-Vink notation [12]:

$$2Bi_{Bi}^{x} + 3O_{O}^{x} = 2V_{Bi}^{'''} + 3V_{O}^{\bullet\bullet}$$

X-ray diffractograms of the prepared samples after the second sintering stage are depicted in Figure (2). It was observed that by increasing the sintering temperature from 720 ºC to 800 ºC, the main $BiFeO_3$ phase is clearly enhanced. The zoom in the 2θ-range of 22º - 33ºillustrated in Figure (2.b) shows clearly the intensities of $BiFeO_3$ phase pronouncedly increases while those of $Bi_{25}FeO_{40}$ phase decreases with no considerable change of $Bi_2Fe_4O_9$ phase as the temperature of the second sintering is ascended to 800ºC. The sample has been melted as sintering temperature ascended above of 800 ºC. Thus, the optimum sintering conditions to synthesize $BiFeO_3$ phase were selected to be at 600ºC and 800ºC for 6hr, for the first and second sintering stages, respectively.

Quantitative phase analysis (QPA) was performed to check the validity of phase optimization parameters. The Rietveld refinement was applied for structural analysis and QPA using MAUD software. Reitveld plotsare given in Figures (3 and 4). QPA results are given in Table (1).The QPA results matches the interpretation of optimization process as given above. Rietveld quantitative phase analysis proved that thehighest abundance of $BiFeO_3$ phasecan be obtainedusing the optimum preparation conditions oftemperature and time of 600ºCand 800ºC for 6hr,for the first and second sintering stages, respectively.

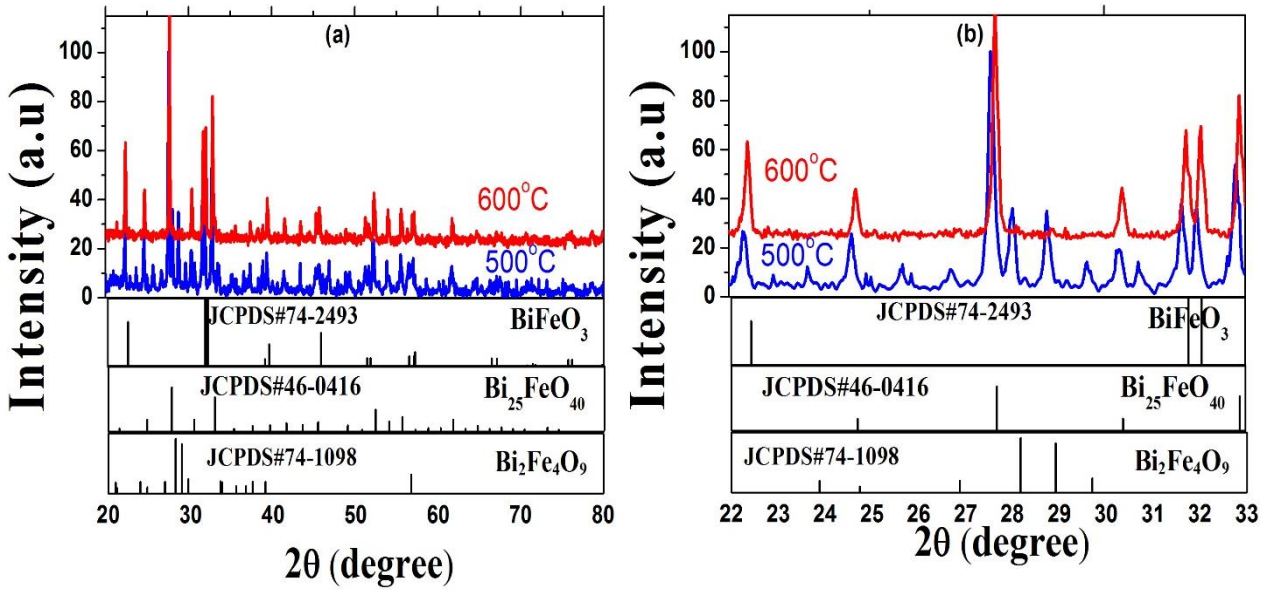

Fig.1: XRD diffractograms of bismuth ferrite samples after the first sintering stage:

a) 2θ = 20-80º) and b) Zoom in region of 2θ = 22-33º (JCPDS cards are illustrated in the figure).

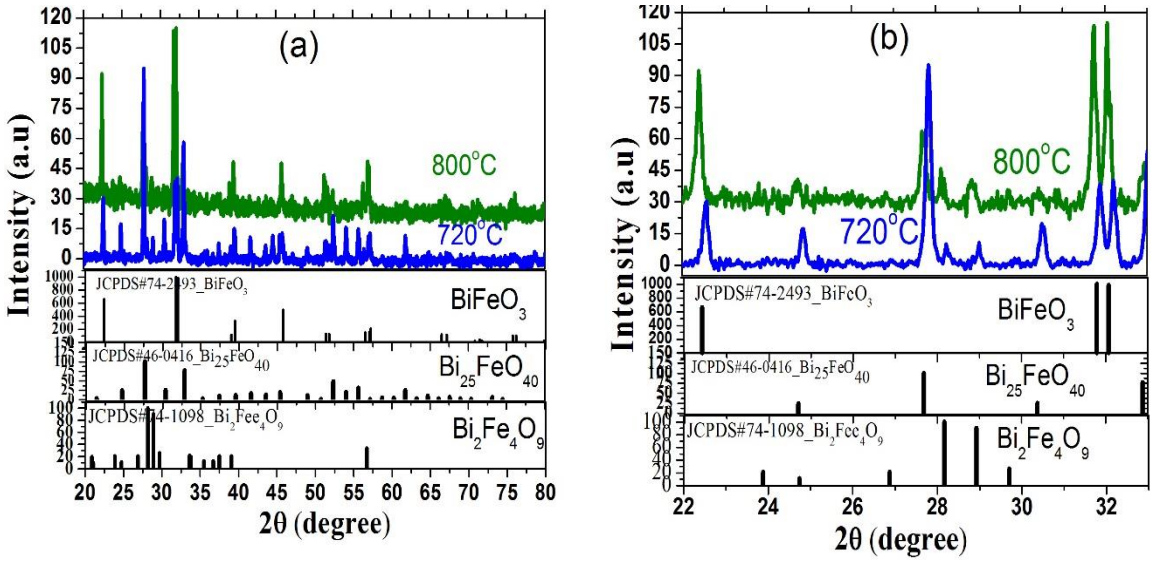

Fig.2: diffractograms of bismuth ferrite samples after the second sintering stage:

a) 2θ = 20-80º) and b) Zoom in region of 2θ = 22-33º (JCPDS cards are illustrated in the figure).

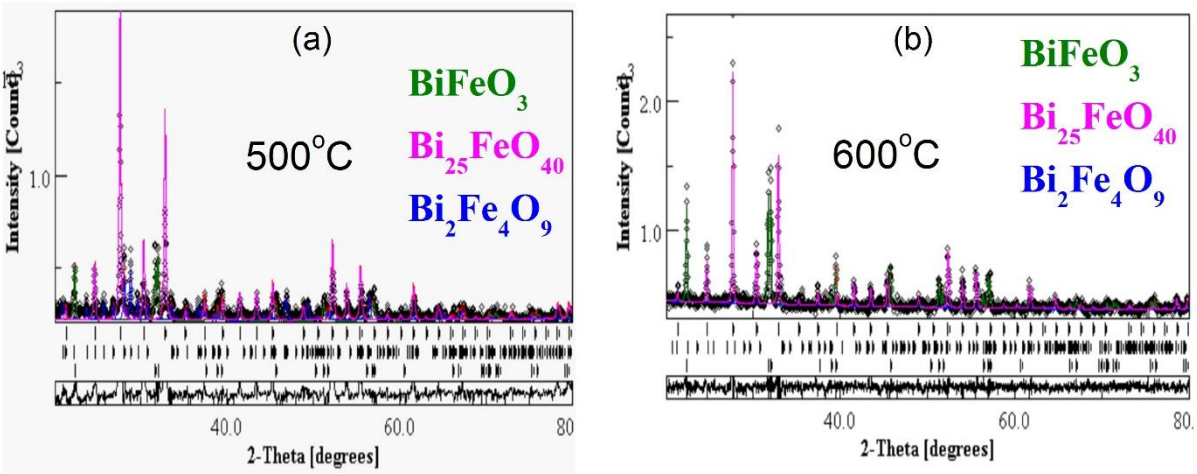

Fig.3: Reitveld plots of bismuth ferrite samples after the first sintering stage.

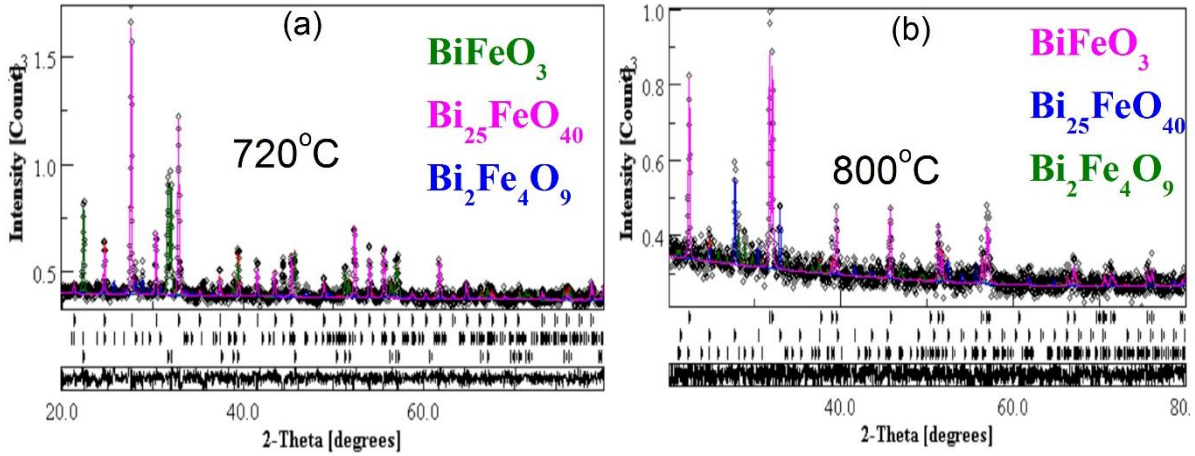

Fig.4: Reitveld plots of bismuth ferrite samples after the second sintering stage.

Table 1: Quantitative phase analysis.

Sintering stage	Temperature (°C)	Phaseconcentration (%)		
		$BiFeO_3$	$Bi_{25}FeO_{40}$	$Bi_2Fe_4O_9$
First	500	22.49	35.96	60.45
	600	42.70	55.48	1.80
Second	720	35.75	49.42	14.82
	800	61.27	16.15	22.56

Raman active mode of ceramic bismuth ferrite (BFO) was shown in Figure (5).The spectrum shows 7 Raman active modes of $BiFeO_3$ phase.The Raman spectra of the synthesized BFO sample was checked through the comparison with previous literature works as shown in Table (2), which confirms the higher quality of BFO as compared.

The electrical and magnetic properties of selected $BiFeO_3$ sample were studied by using, respectively,the two-point contact method and superconducting quantum interference device (SQUID), MPMS3 company, USA.The electrical resistance of bismuth ferrite as a function of temperature was measured from room temperature up to 600K as depicted in Figure (6). A relaxation of resistance value appears around 600K. This reduction isdue to magnetic order phase transition from anti-ferromagnetic (insulating) to paramagnetic (metallic) phaseat 600°C, this temperature considered to be the Neel temperature of the sample.

Magnetic field dependence of the magnetic moment was recorded by plotting the hysteresis loop under an applied magnetic field up to 7 Tesla to determine the magnetic properties of bismuth ferrite sample. Figure (7.a) shows the hysteresis loop of $BiFeO_3$ sample measured slightly above room temperature at (375K), which agrees with the literature [18]. Despite of the reported antiferromagnetic nature of bismuth ferrite, howeverM (H) hysteresis loop shows a small opening with a few magnetic moment values that provides the presence of weak ferromagnetic behavior.The weak ferromagnetic behaviour in the synthesized ceramic $BiFeO_3$ sample is referred to the spin canting mechanism whereas the Dzyaloshinskii- Moriya interaction appears, causing the spin of electrons to be tilted and not perfectly antiparallel, which results in a small net magnetization.

The temperature dependence of magnetic moment investigation of$BiFeO_3$ samplewas performed under an external magnetic field of 100 Oe as shown infigure (7.b),which shows the typical superparamagnetic behaviour. The enhancement of magnetization at low temperature reflects the spin freezing state of the free carriers.

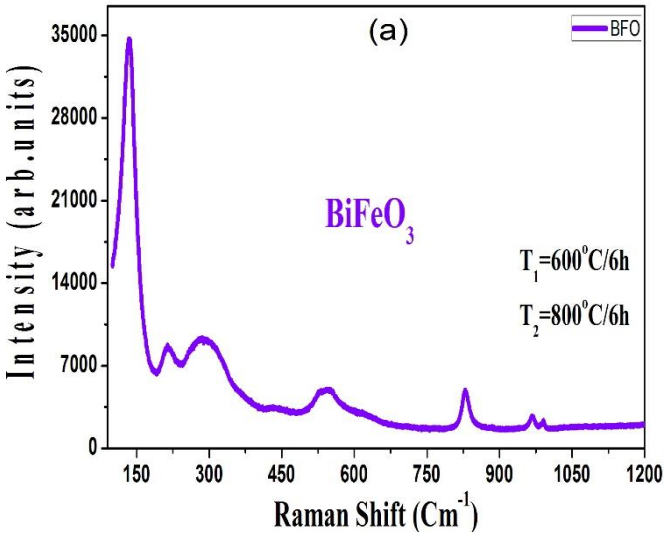

Fig. 5: Raman spectroscopy of pristine bismuth ferrite sample($BiFeO_3$)

Table 2: Raman active modes in this study and previous literature works.

This work	Chaturvedi et al.[13]	R. Palaiet al. [14]	Fukumura et.al. [15]	Singh et al. [16]	Raman mode
137	-	140	147	136	A_1
215	235	200	227	211	A_1
282	268	250	265	275	E
540	521	580	525	549	E
824	-	850	-	-	E
970	-	950	-	-	E
995	-	-	-	-	E

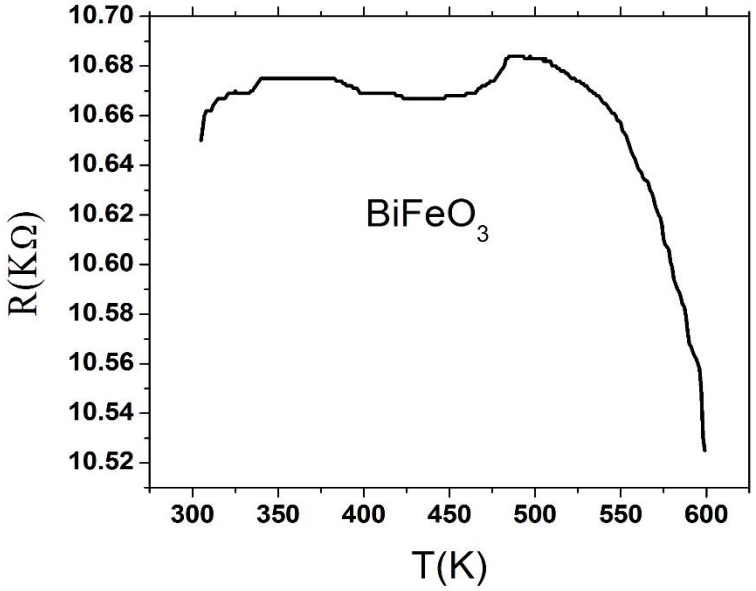

Fig.6: temperature dependence of electrical resistance of BFO.

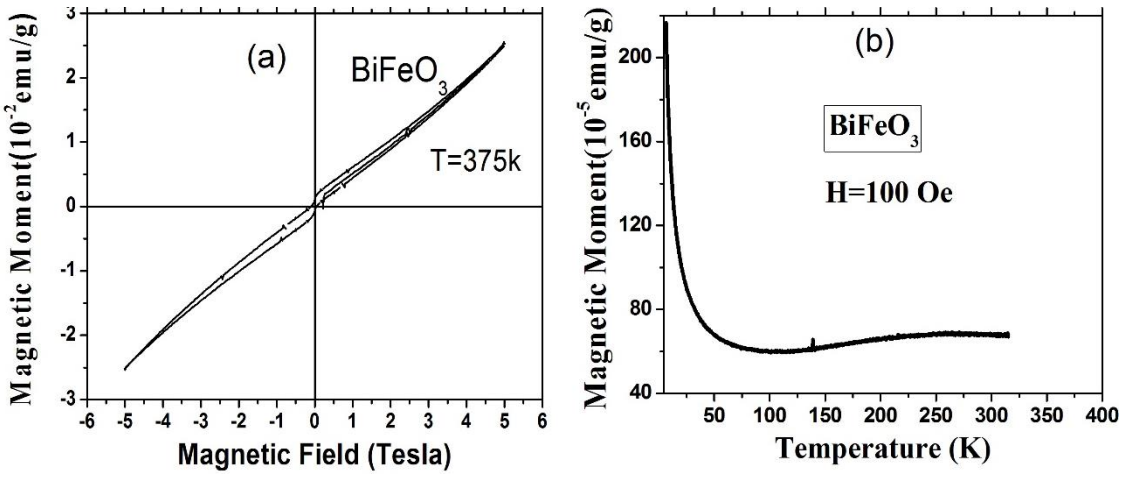

Fig.7: Magnetic moment:a) Magnetic field dependence and b) Temperature dependence of parent BFO sample.

4 Conclusions

$BiFeO_3$phase can be synthesized in considerable concentration using solid state reaction and two sintering stages. Quantitative phase analysis using Reitveld refinement prove thatthe optimum preparation parameters are600^oC and800 ^oC for 6 hr for the first and second stage, respectively. Raman spectroscopy confirms the formation of the structural phase of $BiFeO_3$ sample. A room temperature, weak ferromagnetic behaviour was observed in $BiFeO_3$ sample and it was attributed to the spin canting mechanism.

canting mechanism whereas the Dzyaloshinskii- Moriya interaction appears, causing the spin of electrons to be tilted and not perfectly antiparallel, which results in a small net magnetization.

The temperature dependence of magnetic moment investigation of$BiFeO_3$ sample was performed under an external magnetic field of 100 Oe as shown infigure (7.b),which shows the typical super paramagnetic behaviour.

The enhancement of magnetization at low temperature reflects the spin freezing state of the free carriers.

Acknowledgments: M. I. Marzouk thanks T. Fix, (ICUBE) for his help during the M. Sc. internship at Strasbourg University, Strasbourg, France.

References

[1] M.I. Morozov,N. Lomanova, V. V. Gusarov, Russ. J. Gen. Chem., **73**, 1676–1680 (2003).
[2] G. Catalan, J F. Scott, J. Adv. Mater., **21**,2463 (2009).
[3] E. Jartych, T. Pikula, K. Kowal, J. Dzik, P. Guzdek, D. Czekaj, Nanoscale Res Lett.,**11**, 234, (2016).
[4] S. M. Selbach,M. A. Einarsrud, T. Grande, Chem. Mater., **21**(1), 169 (2009).
[5] C. Ederer and C. Fennie, Journal of Physics Condensed Matter., **20(43)**, 434219 (2008).
[6] N. Maso, A. West, Chem. Mater., **24**, 2127 (2012).
[7] J. R. Carvajal, T. Roisnel, International Union for Crystallography, Newsletter., **20**, (1998).
[8] S. Matthies, J. Pehl, H. R. Wenk, L. Lutterotti, S. C. Vogel, J. Appl.Cryst., **38(3)**, 462(2005).
[9] M. D. Casper, M. D. Losego, J. P. Maria, J. Mater Sci., **48**, 1578(2013).
[10] T. Quickel, L. Schelhas, R. Farrell, N. Petkov, V. Le, S. Tolbert,Nat.Commun.,**6**,7562(2015).
[11] N. Hur, Nature., **429**, 392 (2004).
[12] F. A. Kröger, H. J. Vink, Sol. Stat. Phys., **3**, 307 (1956).
[13] S. Chaturvedi, R. Das, P. Poddar, S. Kulkarni,RSC Adv., **5**, 23563 (2015).
[14] M.K. Singh, H.M. Jang, S. Ryu, M.H. Jo, Appl. Phys. Lett., **88**, 042907 (2006).
[15] H. Fukumura, S. Matsui, H. Harima, T. Takahashi, T. Itoh, K. Kisoda, M. Tamada, Y. Noguchi, M. Miyayama,J. Phys.: Condens. Matter., **19** ,365224 (2007).
[16] R. Palai, J. F. Scott, R. S. Katiyar, Phys.RevB., **81**, 024115(2010).
[17] K. Moma , F. Izumi, VESTA 3 for three-dimensional visualization of crystal, volumetric and morphology data, J. Appl. Cryst., **44**, 1272 (2011).
[18] R. Mazumder, P. Sujatha Devi, D. Bhattacharya, P. Choudhury, A. Sen, Appl. Phys. Lett., **91**, 062510 (2007).